FINAL

PROGRESS REPORT

Covering Period from
15 March 1967 to 15 ~~October~~ March 1968

RADIATION DAMAGE TO SEMICONDUCTORS BY HIGH ENERGY ELECTRONS

John C. Corelli

Sponsored by the National Aeronautics and Space Administration

Under Grant NsG 290

Division of Nuclear Engineering and Science

Rensselaer Polytechnic Institute

Troy, New York

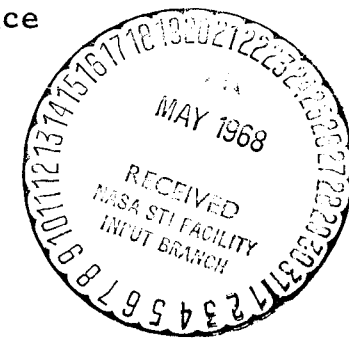

I. Introduction

In this final report we shall briefly summarize the progress of research work conducted in the period 15 April 1967 to 1 February 1968 on NASA Grant NsG-290*. A portion of the research work formerly sponsored under the Grant (NsG-290) is now included under NASA Grant NGR 33-018-090**. In the latter program we have been concentrating on the interactions of lithium impurities with radiation - induced defects, and the original research program of Grant NsG-290 has been factored into the lithium - associated defects research program.

The following personnel were actively engaged in the research program.

Faculty: Dr. John C. Corelli (half time)

Research Technician: Mr. James W. Westhead

Graduate Students: Mr. Arne H. Kalma (NASA Traineeship)

Mr. William Bohlke (left June 1, 1967 with M. S. Degree)

Mr. Robert J. Edelstein (summer only 1967)

The program supported the doctoral research program of Mr. Arne H. Kalma*** which was completed in January 1968. The Ph.D. thesis submitted by Mr. Kalma was titled:

---

* Mr. Roger A. Breckenridge, NASA Langley Research Center, Hampton, Va., was the technical monitor for Grant NsG-290

** Dr. Paul H. Fang, NASA Goddard Space Flight Center, Greenbelt, Md., is the technical monitor for Grant NGR 33-018-090.

*** Will spend one year 1 April 1968 to 1 April 1969 as a post doctoral research fellow at the Univ. of Paris, École Normale Superiéure, Laboratoire de Physique, Paris, France.

"Photoconductivity Including Stress-Induced Dichroisim of Defects in Silicon"

A paper based on the thesis is being submitted for publication in the Physical Review. Some of the Photoconductivity studies in electron-irradiated silicon were reported at the Santa Fe Conference on Radiation Effects in Semiconductors 3-5 October 1967 and the proceedings will be published by Plenum Press (1968).

PHOTOCONDUCTIVITY STUDIES OF DEFECTS IN SILICON USING STRESS-INDUCED DICHROISM TECHNIQUES

A. Introduction

In our last progress report, preliminary photoconductivity studies were presented. Since then we have carried out extensive experiments including stress - induced dichroism studies of divacancy associated energy levels in irradiated silicon. These experiments formed the basis of the Ph.D. thesis of A. H. Kalma entitled "Photoconductivity Including Stress - Induced Dichroism of Defects in Silicon." This report will be a brief review of the results obtained in these studies.

B. Experimental Description

All samples used in this study were low oxygen containing ($\lesssim 10^{16}$ e/cm^2) zone-refined material. The n-type material was 1 ohm-cm and the p-type material was 100 ohm-cm and 7100 ohm-cm. The samples were irradiated with both 1.5 MeV and 50 MeV electrons.

The spectrometer used to provide monochromatic light was a Perkin-Elmer model 98 monochromator equipped with a LiF prism. An airtight box was built around the monochromator and dry nitrogen was used to purge the apparatus.

The optical cryostat used for the application of low temperature stress has been briefly described in the previous progress report. The cryostat tail piece with the sample holder are shown in Fig. 1. Indium foil was placed at both ends of the sample to fill in roughness and to allow for slight devia-

tions from parallel of the planes at both ends. Figure 2 shows the cryostat top. The platform insured that the stress was applied directly downward on the center rod. The force was applied by lead shot hung in a bucket on the end of a rod that achieved a force multiplication factor of six. The whole inner tube and rod were raised one inch before stressing so that the sample was above the cold windows in case the sample shattered.

C. Results and Discussion

In n-type material irradiated with 1.5 MeV electrons, energy levels located at E_c-0.39 eV and E_c-0.54 eV have been identified as being associated with transitions from the divacancy.

The technique of measuring the stress - induced dichroism allows determination of several things. By determining the sense of the dichroism for various stress and incident light directions, the configuration of the defect can be deduced. We have found that the defect giving rise to the E_c-0.39 eV and E_c-0.54 eV level has an atomic symmetry around a $\langle 111 \rangle$ direction and a transition dipole along a $\langle 110 \rangle$ direction.

Also, the energy level shape can be determined from the dichroism measurement. By requiring that the energy level shape be the same for each light polarization and also for the difference in the spectra measured with different light polarizations and in addition requiring that the dichroism of the energy level be the same at all energies, the energy level shape

of the level in question is determined. This method is illustrated in Figure 3 where the energy level shape of both E_c-0.39 eV and E_c-0.54 eV are shown. Both levels have a sharp initial rise in ionization and electrons are ionized from them at all energies higher than the initial ionization energy. (Quoted energy level positions are taken to be the energy at which ionization first takes place.) This energy level shape suggests the conclusion that the transitions responsible for the photoconductivity are from defect states to the conduction band.

The activation energy of the E_c-0.39 eV level was determined to be 1.25 eV by isothermal annealing experiments. Both the E_c-0.39 eV and E_c-0.54 eV levels annealed out isochronally in the temperature region around 300°C. The atomic stress-induced reorientation annealed out isochronally at 150°C. The two levels are independent of chemical species (As, Sb, or P) of dopant. If the Fermi level was above $\sim E_c$-0.22 eV, the E_c-0.54 eV level was not observed and the E_c-0.39 eV level was. If the Fermi level was below $\sim E_c$-0.22 eV, only the E_c-0.54 eV level was observed. However, if white light was shone on the sample at the same time that the spectrum was measured, both levels were observed. (The sample shown in Fig. 3 had the Fermi level near $\sim E_c$-0.22 eV so both levels were observed.)

These results lead to the conclusion that the E_c-0.39 eV and E_c-0.54 eV levels are associated with the doubly negative and singly negative charge states of the divacancy respectively.

The photoconductivity band centered at 3.9 microns in irradiated p-type silicon has been identified by Cheng[2,3] as being associated with the singly positive charge state of the divacancy. Due to the shape of the band, he has explained it as an excitation from the ground state to an excited state of a defect followed by decay of a hole from the empty ground state to the valence band. The samples used by Cheng were boron doped. We have observed this same band in nominally undoped, 7100 ohm-cm silicon after irradiation and subsequent annealing. This is shown in Fig. 4.

The reason that the band was not seen immediately after irradiation in this high resitivity material is that the Fermi level was too high. The band is only observed if the Fermi level is closer to the valence band than $\sim E_V+0.26$ eV.

The observation of the 3.9 micron photoconductivity band in undoped, p-type silicon strengthens the conclusion that it is associated with the divacancy.

The dominant defect photoconductivity observed in 45-50 MeV electron-irradiated silicon has been found to be an "energy band" that extends from the band edge down to an energy of about 0.3 eV. This is in contrast with 1.5 MeV electron irradiations where the dominant defect photoconductivity was produced by single levels. These two different effects are shown in Fig. 5.

A reasonable explanation of the difference is that 45 MeV electrons produce disordered regions in silicon and 1.5 MeV

electrons do not. These disordered regions would destroy some of the lattice periodicity which would have the effect of destroying the sharp division between the forbidden and allowed energies at the band edges. This would put a continuous spectrum of allowed energies in the forbidden gap extending from the band edges into the gap. Simple defects induced by 1.5 MeV electrons are also disorder of a sort and would cause the same effect but to a much lesser degree than the 45 MeV electron induced disordered regions. The "energy band" observed in 1.5 MeV electron irradiated samples extends only down to about 0.8 eV and is much smaller in magnitude that is the case for 45 MeV electrons.

Following the suggestion of Vavilov,[4] we have drawn a schematic to represent the measured decrease in forbidded gap energy resulting from 45-50 MeV electron irradiations.

Schematic diagrams of the forbidden gap change of shape are given for 1.5 MeV and 45 MeV electrons.

EFFECT OF 50 MeV ELECTRONS ON THE ULTIMATE FERMI LEVEL IN GERMANIUM

This work has been written up in a paper submitted for publication in the Journal of Applied Physics. Here we shall give only the abstract of the paper since preprint copies have been submitted to NASA previously. (27 October 1967).

P-type germanium doped with gallium and indium to resistivities ranging from 0.001 to 30 ohm-cm and n-type germanium doped with antimony and arsenic to resistivities ranging from 0.1 to 30 ohm-cm were irradiated with 50 MeV electrons to various doses up to a maximum total integrated flux of 1.0×10^{19} e/cm^2. Electrical measurements were performed to determine the effect of irradiation on the temperature dependence (78 to $320^{o}K$) of the conductivity, carrier concentration, and Fermi level. After irradiation to relatively high doses ($\gtrsim 10^{18}$ e/cm^2) both types of germanium reach a saturation in the hole concentration which is accompanied by an ultimate value for the Fermi level at $E_V + 0.220 \pm 0.010$ eV for all samples studied. Comparison of this result with studies made using 10 MeV deuterons and fast neutrons shows that the position of the ultimate Fermi level strongly depends on the damaging or "disordering" capabilities of the incident radiation. We find that the ultimate Fermi level is positioned closer to the valence band as a result of irradiation by particles capable of imparting a larger maximum recoil energy to the germanium atom. Finally, a comparison is made for germanium irradiated by Co^{60} gamma rays and 4.5 MeV electrons which do not produce disordered

regions and it is found that the ultimate Fermi level is pinned to a single level at $E_v + 0.25$ eV for Co^{60} gamma rays and at $E_v + 0.22$ eV for electrons.

INFRARED ABSORPTION STUDIES OF 45-50 MeV ELECTRON IRRADIATED HEAVILY DOPED SILICON

This work was started within the past year and has been discontinued for the present time because of program termination.

The research work involved in this study was to determine the impurity associated radiation-induced defects by infrared spectrosocopy measurements on silicon samples doped to relatively high concentrations with Bi, As, B 0, and P. The resistivity range studied was from 0.1 to 0.01 ohm-cm. The samples were irradiated to total integrated 45-50 MeV electron fluxes of $\sim 2 \times 10^{18} e/cm^2$ with the sample temperature kept at $\approx 320^{o}K$ during exposure. All infrared spectra were measured at $80^{o}K$ in the work to be reported.

In Fig. 7 is shown the infrared spectra for a 0.01 ohm-cm phosphorus doped silicon sample (Floating Zone) before anneal and after 15 minute anneals at $135^{o}C$ and at $145^{o}C$. The marked decrease in transmission after the heat treatments arises characteristically from absorption by free carriers which are released from radiation-induced defect traps upon anneal. The large absorptions in the range 2600 cm-1 to 3650 cm^{-1} (curve marked "$135^{o}C$") are in the wavelength region of the spectrum where the infrared absorption bands due to the divacancy defect

are observed.[5] Results similar to those shown in Fig. 7 were also obtained for the 0.01 Ω-cm Bi-doped pulled silicon crystals. Since no further work has been done on these samples we can not conclude that a radiation-induced impurity-associated band is formed in the 2.5μ to 50μ wavelength range. However, it is clear from the results of Fig. 7 that some impurity dependent absorption may be present between 2600 cm^{-1} to 3500 cm^{-1} since we never observed such large absorptions in similar irradiations with silicon containing $\gtrsim$ 100 times higher donor impurity concentration

The well known[6,7,8] radiation-induced oxygen-vacancy complex in silicon (the A-center) gives rise to a vibrational absorption band at 832 cm^{-1}. The 832 cm^{-1} band is only observed in high oxygen-containing ($\gtrsim 10^{17} cm^{-3}$) silicon which is pulled from the melt without further refinement. In Fig. 8 is shown the spectrum of a 0.01Ω-cm bismuth-doped pulled silicon sample V-2 after irradiation but before any heat treatment. The only absorption band of interest to us is the radiation-induced band at 832 cm^{-1} the so-called A-center band. The band at 1125 cm^{-1} is the normal oxygen-interstitial vibrational band while the band at 518 cm^{-1} is due to an electronic transition from the 1S state of the bismuth donor impurity, the other bands are normal lattice vibrational bands which are characteristic of the silicon lattice.

The sample whose spectrum is given in Fig. 8 was subjected to 15 minute heat treatments at the following temperatures (in degrees centigrade) 104, 116, 128, 140, 152, 165, 204, and 250.

In Fig. 9 we show the spectrum measured on sample V-2 after the 15 minute heat treatment at 250°C. We now find that a new band at 882cm^{-1} has evolved and the 832cm^{-1} absorption band has decreased in intensity. The decay and growth of oxygen-associated defect bands is now well known for both silicon [6,7,8] and germanium,[9,10] and reflects the complex structures that are produced by defects (vacancies, interstitials impurities etc.,) as they migrate through the lattice and interact with impurities. The significant result given in both Figs. 8 and 9 is the large pronounced absorption of the defect bands at 832 cm^{-1} and at 882 cm^{-1} compared to the magnitude of the absorption of the normal oxygen impurity band at 1125 cm^{-1}.

In Fig. 10 we show the spectrum from 400 cm^{-1} to 1200 cm^{-1} of a pulled Bi-doped (0.01 ohm cm) silicon sample (V-2) after 15 minutes at each of the temperatures shown. The sample was irradiated at 300°K to a total dose of 2×10^{18} e/cm^2 (48 MeV electrons). The absorption bands at 735 cm^{-1} and 612 cm^{-1} are well-known lattice bands of silicon, while the band at 1125 cm^{-1} is characteristic of pulled silicon and represents the vibrational band of interstitial oxygen in silicon. The absorption band at 511 cm^{-1} is characteristic of the bismuth donor[11] transition 1S→2p. Our main concern will be to focus on the bands at 882 cm^{-1} and 832 cm^{-1} (A-center). Note that in Fig. 10 the band at 882 cm^{-1} grows upon heat treatment to 204°C. In Fig. 11 we show the spectrum of a pulled Bi-doped sample V-3 cut from the same ingot as the one whose results are presented in Fig. 10 except that the sample was irradiated to a lower dose ($\lesssim 10^{18}$e/cm^2)

of 48 MeV electrons compared to $2x10^{18}$ e/cm^2 for sample V-2. It is most striking to note the disappearence of the A-center at 152°C since many researchers[6,7,8,12] including work performed in our laboratory, has shown that the annealing temperature is 350°C. For same time it was believed that the A-center band was vibrational in nature and appeared in oxygen containing silicon as a radiation-induced defect independent of the position of the Fermi level. The results shown in Figs 10 and 11 do not agree with the conclusion of the Fermi level dependence and quite naturally raise some important basic questions. It is our intention to return to this problem at a later date when funds and manpower are available. We shall not give further conclusions on this finding here.

Figure Captions

Figure 1. Liquid Helium Cryostat Tail Piece with the Sample Holder.

Figure 2. Cryostat Top with the Platform for the Application of Stress.

Figure 3. Dichroism after Stress of 1770 kg/cm^2 at 157°C for 15 Minutes Exhibited by a Phosphorus-Doped, 1 Ohm-Cm Sample Irradiated with 4×10^{16} e/cm^2 at 1.5 MeV.

Figure 4. Isochronal Annealing of a High Resistivity, 7100 Ohm-Cm Sample Irradiated with 10^{16} e/cm^2 at 1.5 MeV.

Figure 5 Contrast Between 1.5 MeV and 50 MeV Electron Irradiated, Phosphorus-Doped, 1 Ohm-Cm Silicon.

Figure 6 Schematic of the Decrease in Forbidden Gap Energy Resulting from 45 MeV and 1.5 MeV Electron Irradiations (Following Vavilov[4]).

Figure 7 Infrared spectra of 0.01 ohm-cm silicon (FZ) p-doped after irradiation by 48 MeV electrons, the spectrum is shown before anneal and after 15 minute heat treatment at 135°C and 145°C.

Figure 8 Infrared spectrum of pulled 0.01 ohm-cm Bi-doped silicon after 48 MeV electron irradiation to 2×10^{18} e/cm^2 (sample V-2) before annealing.

Figure 9 Infrared spectrum of pulled 0.01 ohm-cm Bi-doped silicon after 48 MeV electron irradiation to

2×10^{18} e/cm^2 (sample V-2) after 15 minute annealing at 250°C.

Figure 10 Infrared spectra of pulled 0.01 ohm-cm Bi-doped silicon after 48 MeV electron irradiation and annealing for 15 minutes at each of the indicated temperatures. (sample V-2)

Figure 11 Infrared spectra of pulled 0.01 ohm-cm Bi-doped silicon after 48 MeV electron irradiation to $\lesssim 10^{18}$e/cm^2 and annealing for 15 minutes at each of the temperatures indicated.

Literature Cited

1. A. H. Kalma, Ph.D. thesis, Rensselaer Polytechnic Institute, January, 1968 (unpublished).
2. L. J. Cheng, Phys. Lett., 24A, 729 (1967).
3. L. J. Cheng, paper presented at Santa Fe Conference on Radiation Effects in Semiconductors, Oct. 1967 (proceedings to be published by Plenum Press).
4. V. S. Vavilov, Radiation Damage in Semiconductors. 7th International Conference on the Physics of Semiconductors, Paris-Royaument, 115, Dunod, Paris (1965).
5. L. J. Cheng, J. C. Corelli, J. W. Corbett, and G. D. Watkins, Phys. Rev., 152, p 761 (1966).
6. J. W. Corbett, G. D. Watkins, R. M. Chrenko and R. S. McDonald, Phys. Rev., 121, 1015 (1961); ibid., 135A, 1381 (1964).
7. J. C. Corelli, G. Oehler, J. F. Becker, and K. J. Eisentraut; J. Appl. Phys., 36, 1787 (1965).
8. A. K. Ramdas, and M. G. Rao, Phys. Rev. 142, 451(1966)
9. R. E. Whan and H. J. Stein, Appl. Phys. Letters 3, 187 (1963, see also R. E. Whan Phys. Rev. 140A, 690 (1965).
10. J. F. Becker and J. C. Corelli, J. Appl Phys. 36, 3606 (1965)
11. H. J. Hrostowski, in Chapter 10 of "Semiconductors" edited by N. B. Hannay, 1959.
12. J. C. Corelli, Symposium on Lattice Defects in Semiconductors, Tokyo, 1966, to be published by Gordon Breach, May 1968.

SCALE 2:1

1 ELECTRICAL INSULATION
2 SPRING CONTACTS
3 SAPPHIRE WINDOW
4 NaCl WINDOW
5 SAMPLE HOLDER
6 SAMPLE HOLDER TUBE
7 SAMPLE HOLDER ROD

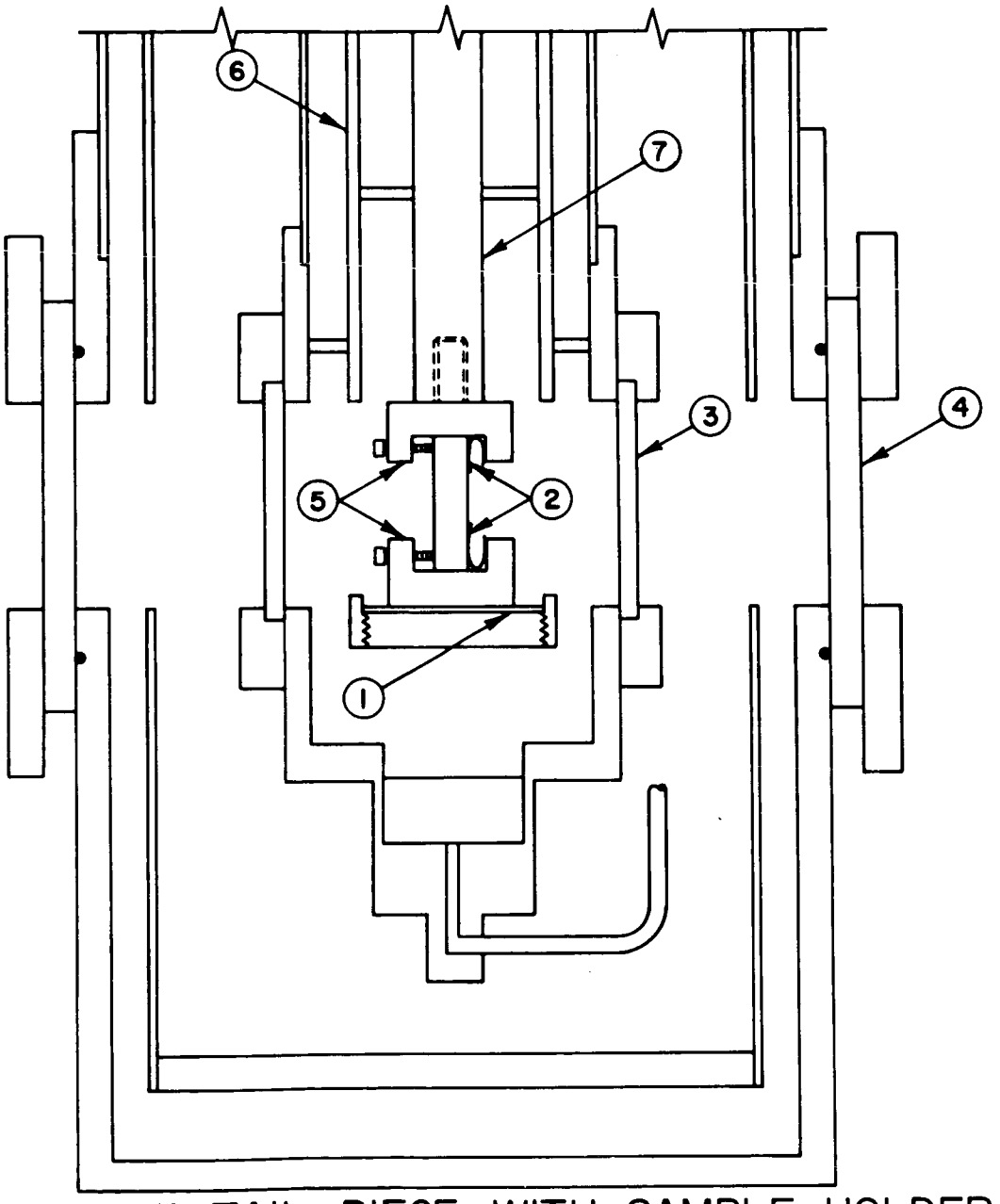

CRYOSTAT TAIL PIECE WITH SAMPLE HOLDER

Fig 1.)

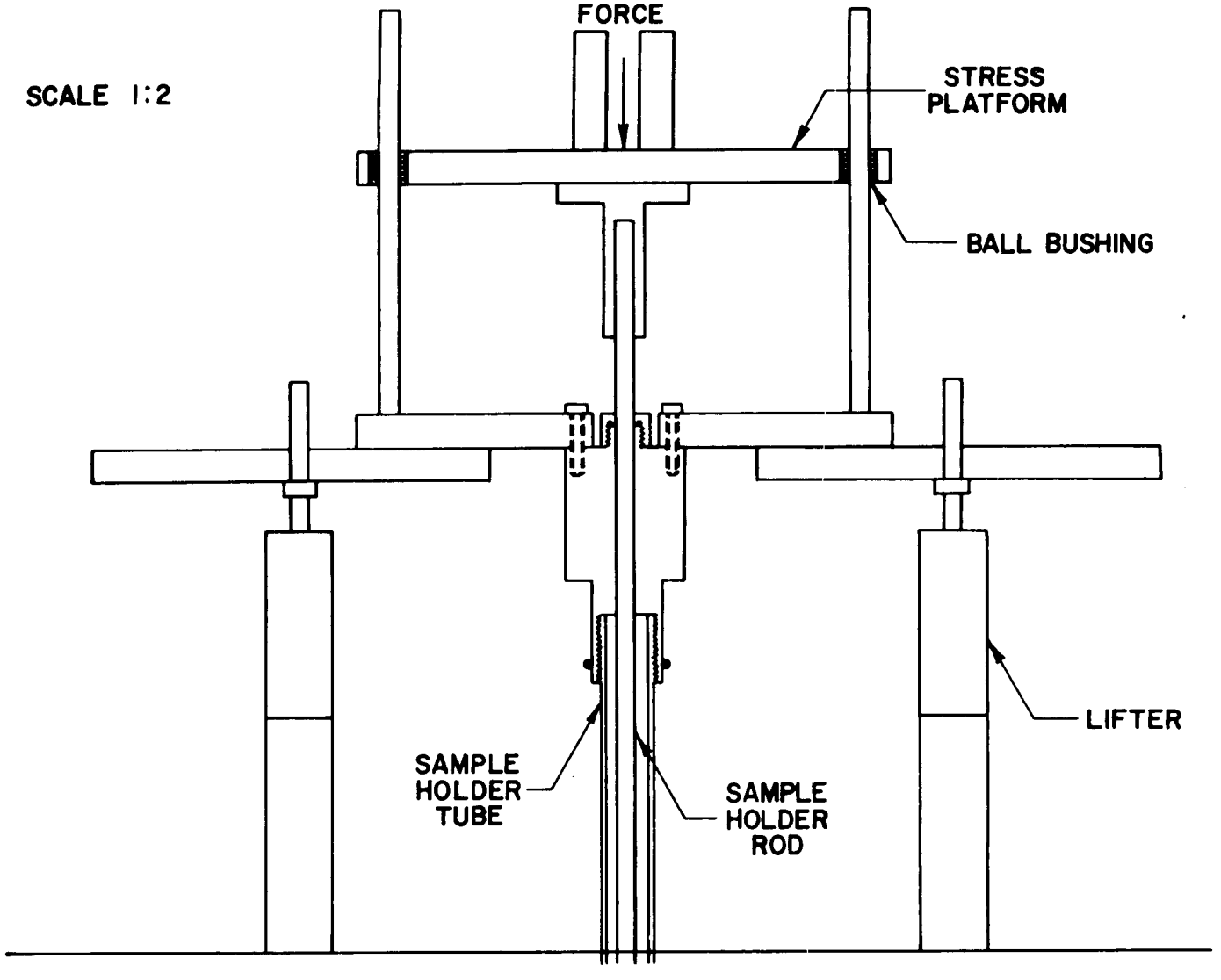

CRYOSTAT TOP FOR STRESS

(2 Fig)

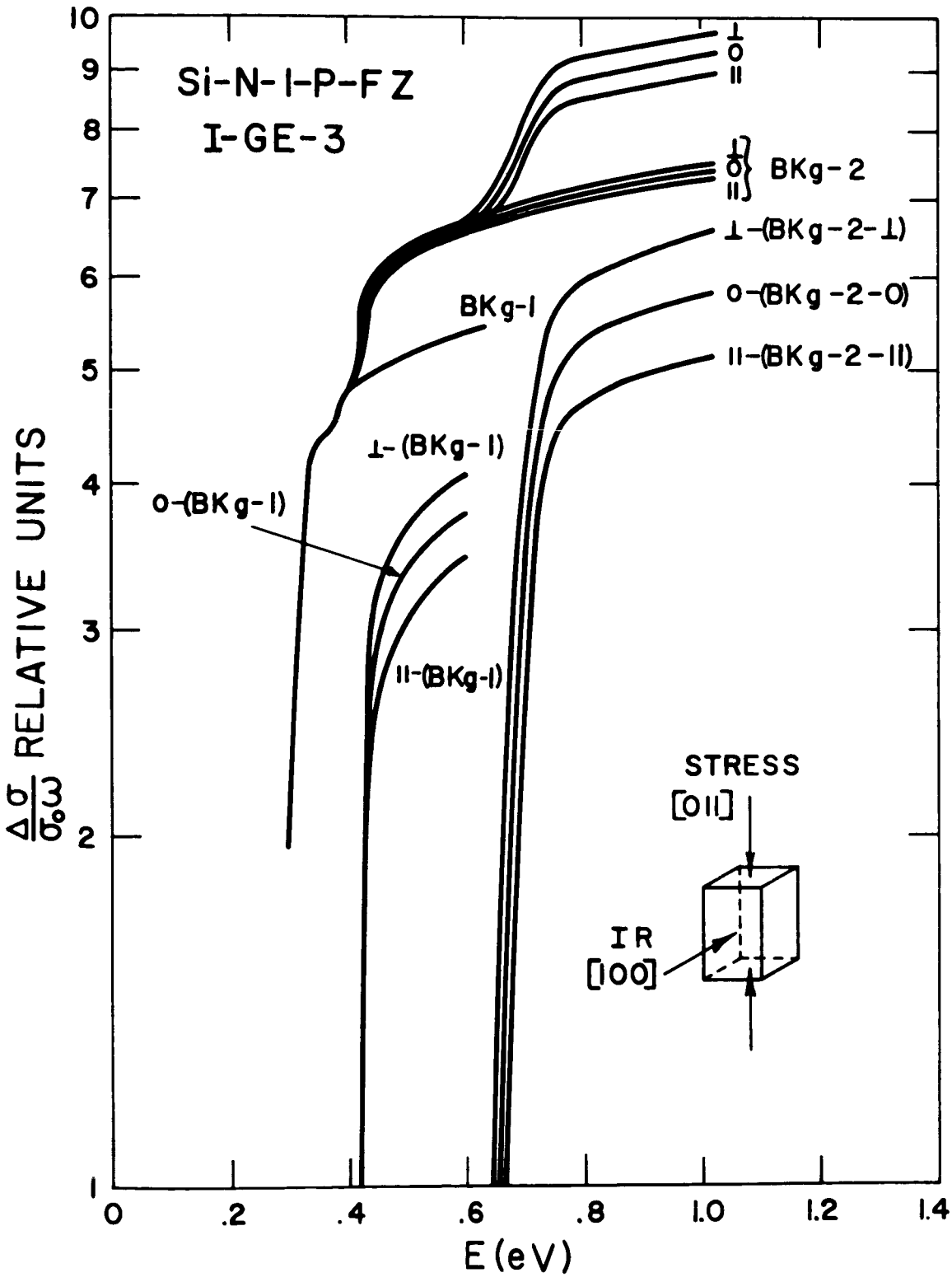
Si-N-I-P-F Z
I-GE-3
BKg-2
BKg-1
⊥-(BKg-2-⊥)
0-(BKg-2-0)
II-(BKg-2-II)
⊥-(BKg-1)
0-(BKg-1)
II-(BKg-1)
STRESS
[011]
IR
[100]
Δσ/σ₀ω RELATIVE UNITS
E(eV)
10
9
8
7
6
5
4
3
2
1
0
.2
.4
.6
.8
1.0
1.2
1.4

Fig 3.)

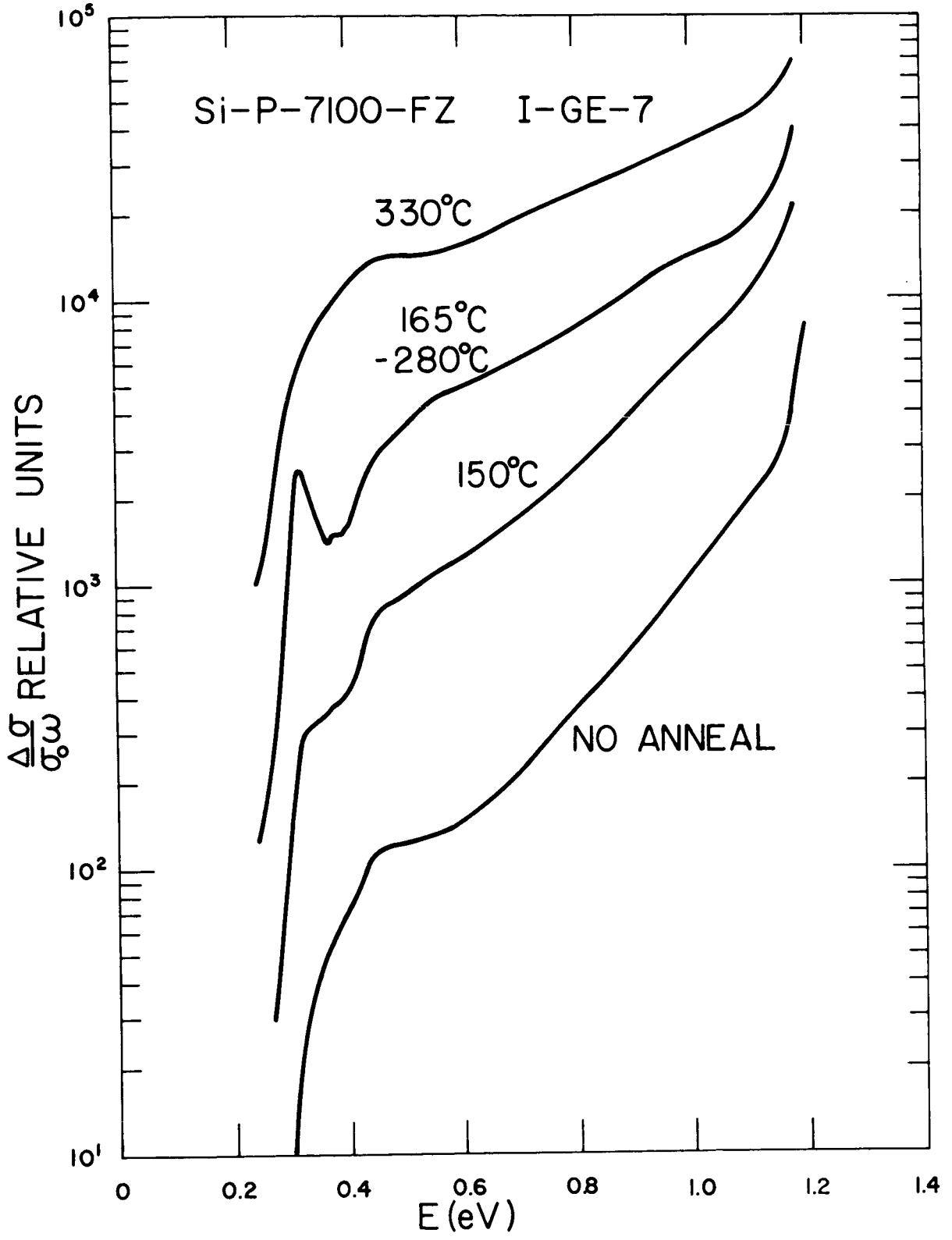
Si-P-7100-FZ I-GE-7
330°C
165°C
-280°C
150°C
NO ANNEAL
$\frac{\Delta\sigma}{\sigma_0\omega}$ RELATIVE UNITS
10^5
10^4
10^3
10^2
10^1
0
0.2
0.4
0.6
0.8
1.0
1.2
1.4
E (eV)

Fig 4)

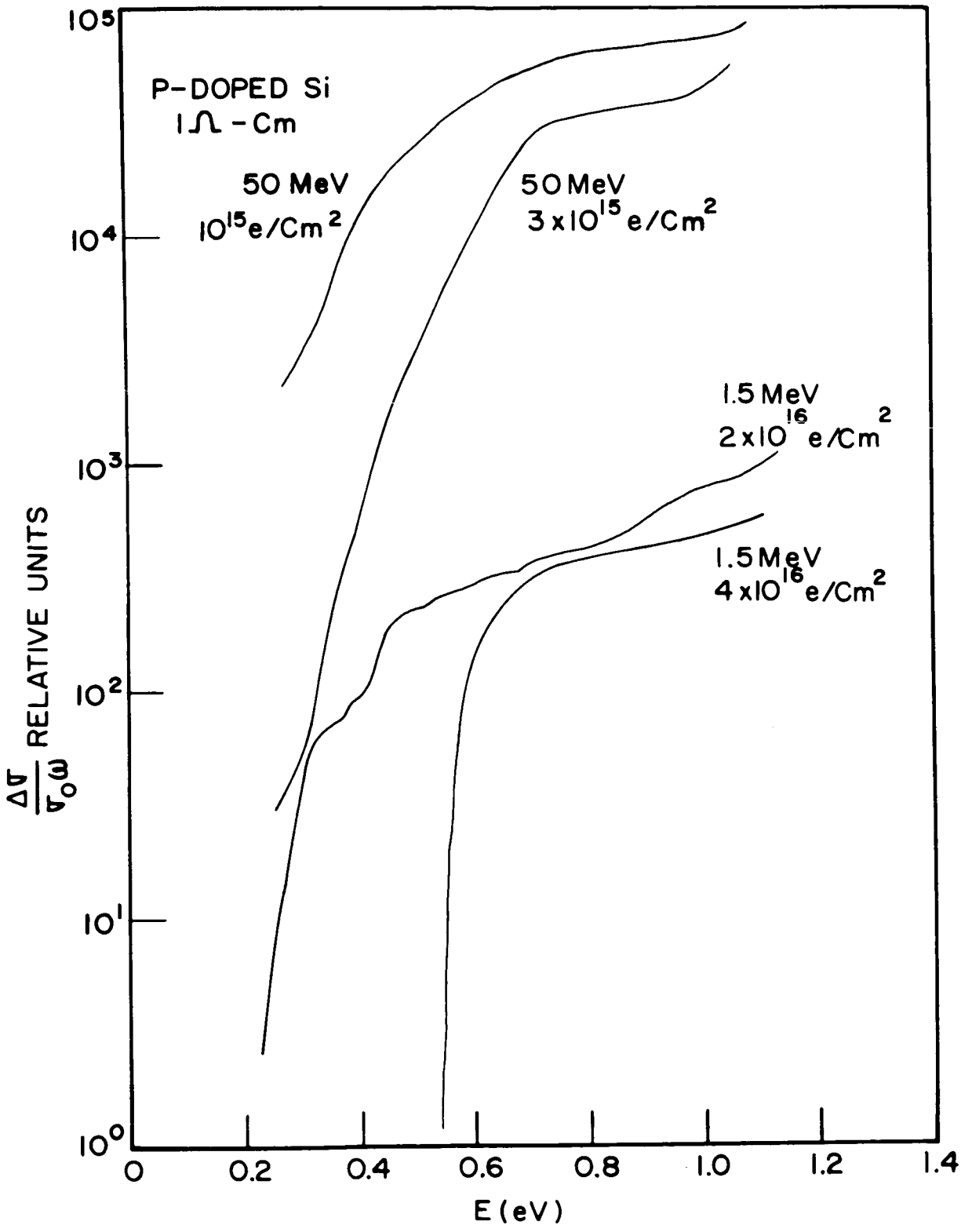
P-DOPED Si
1Ω - Cm
50 MeV
10^15 e/Cm^2
50 MeV
3x10^15 e/Cm^2
1.5 MeV
2x10^16 e/Cm^2
1.5 MeV
4x10^16 e/Cm^2
Δσ/σ0ω RELATIVE UNITS
10^5
10^4
10^3
10^2
10^1
10^0
0
0.2
0.4
0.6
0.8
1.0
1.2
1.4
E (eV)

Fig 5)

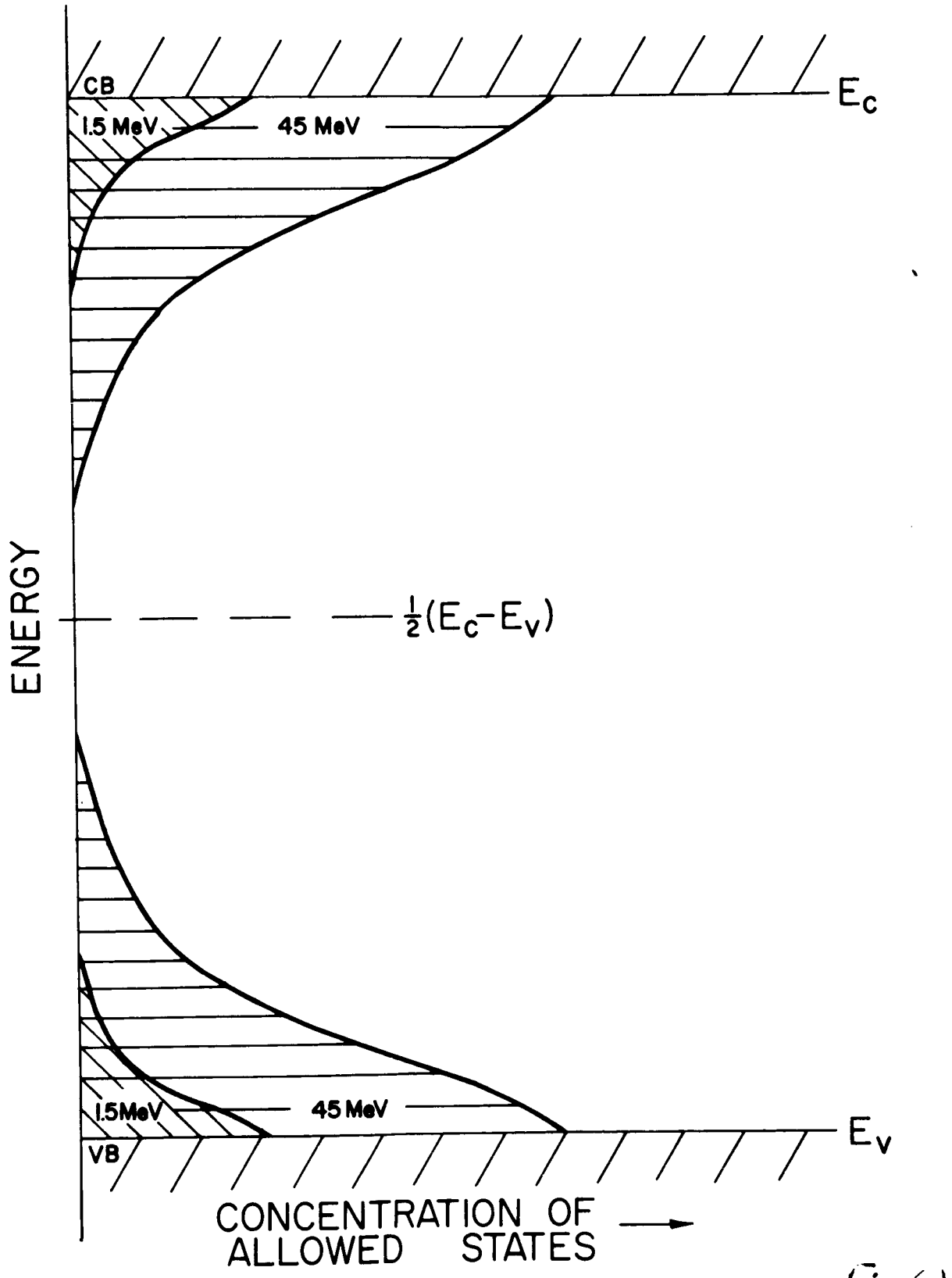
CB
1.5 MeV
45 MeV
E_c
ENERGY
$\frac{1}{2}(E_c - E_v)$
1.5MeV
45 MeV
VB
E_v
CONCENTRATION OF ALLOWED STATES

Fig 6.)

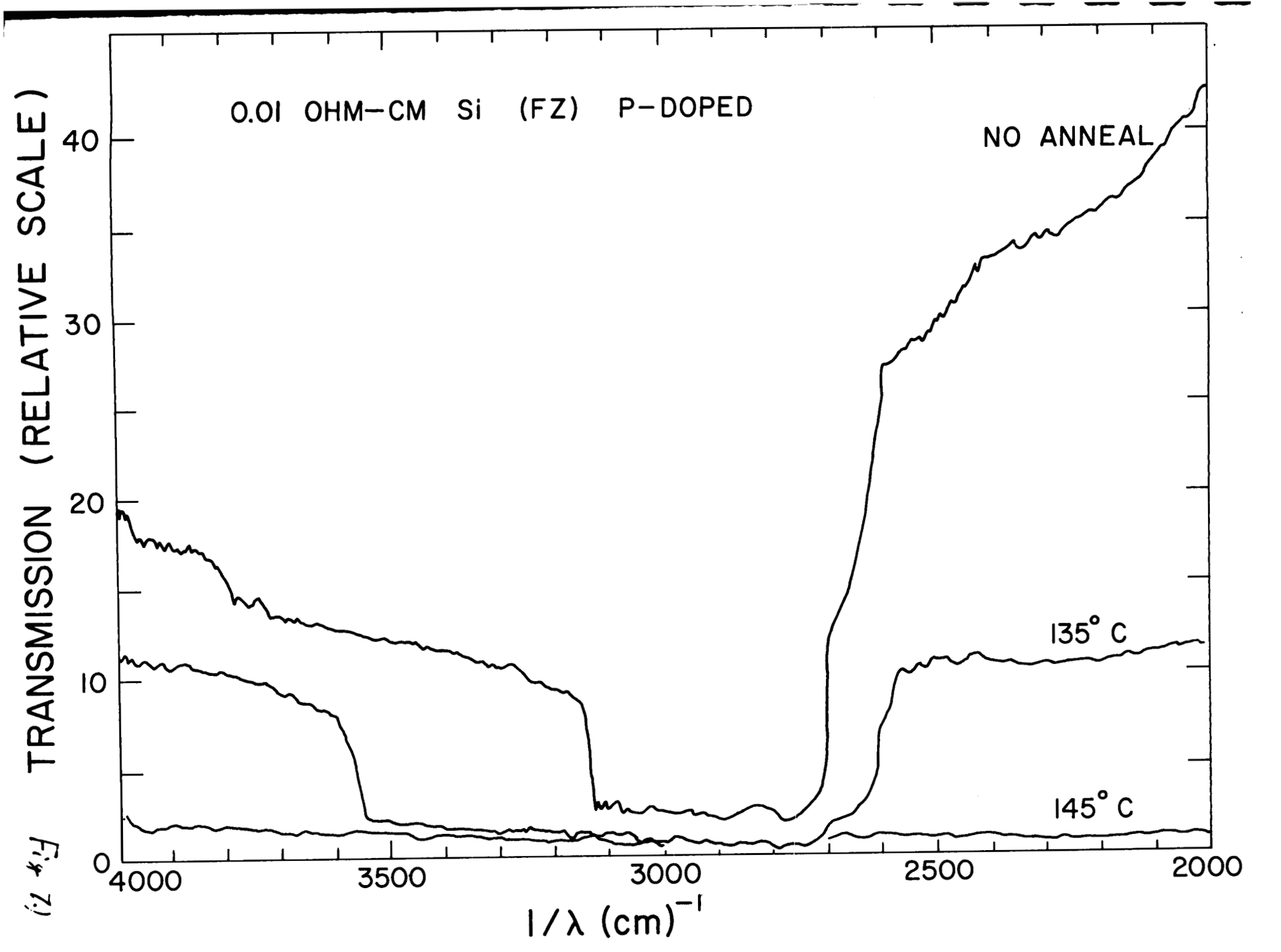
0.01 OHM-CM Si (FZ) P-DOPED
NO ANNEAL
135° C
145° C
TRANSMISSION (RELATIVE SCALE)
0
10
20
30
40
4000
3500
3000
2500
2000
1/λ (cm)⁻¹

Fig 2j

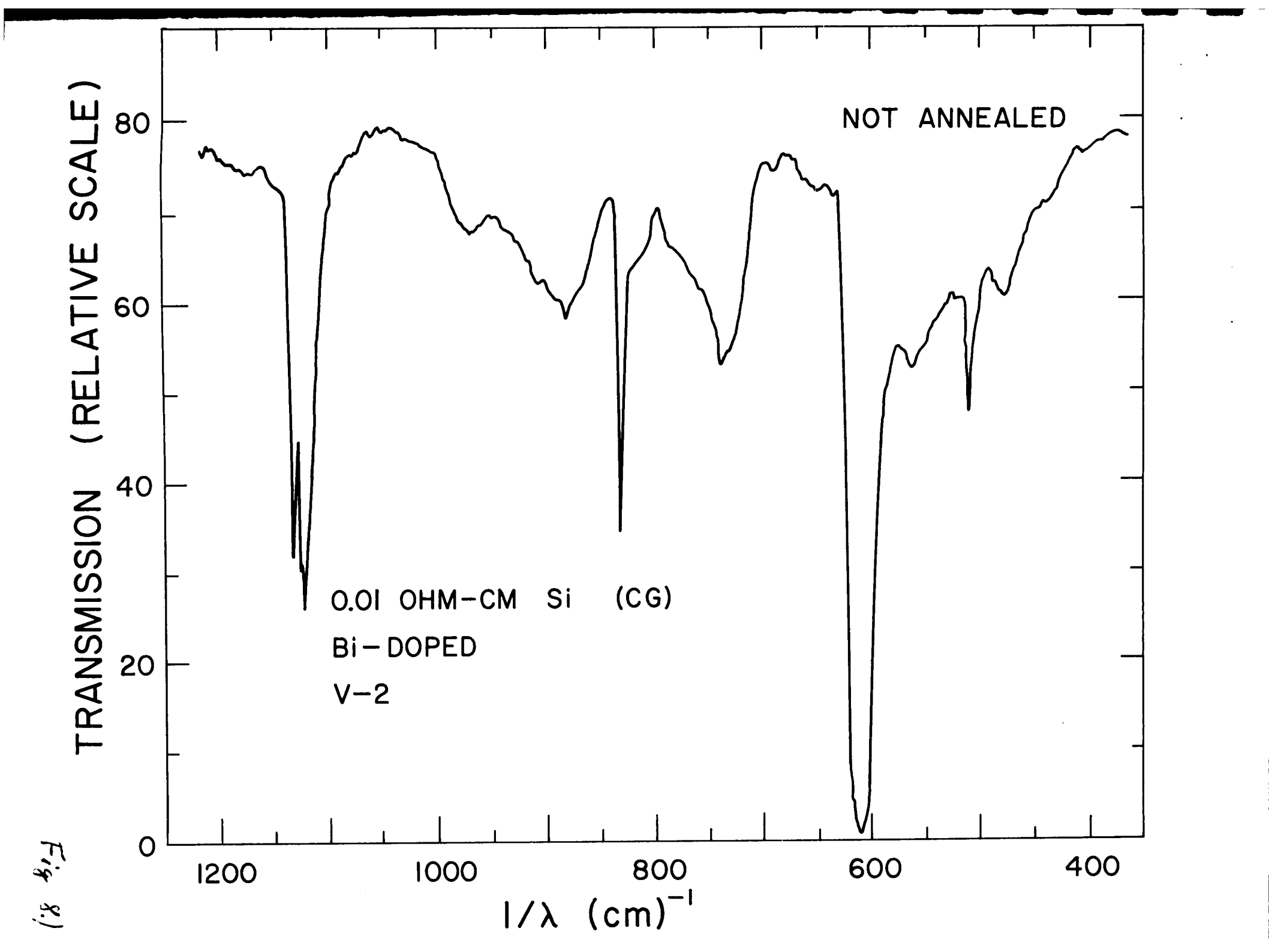
NOT ANNEALED
0.01 OHM-CM Si (CG)
Bi-DOPED
V-2
TRANSMISSION (RELATIVE SCALE)
0
20
40
60
80
1200
1000
800
600
400
1/λ (cm)⁻¹

Fig 8j

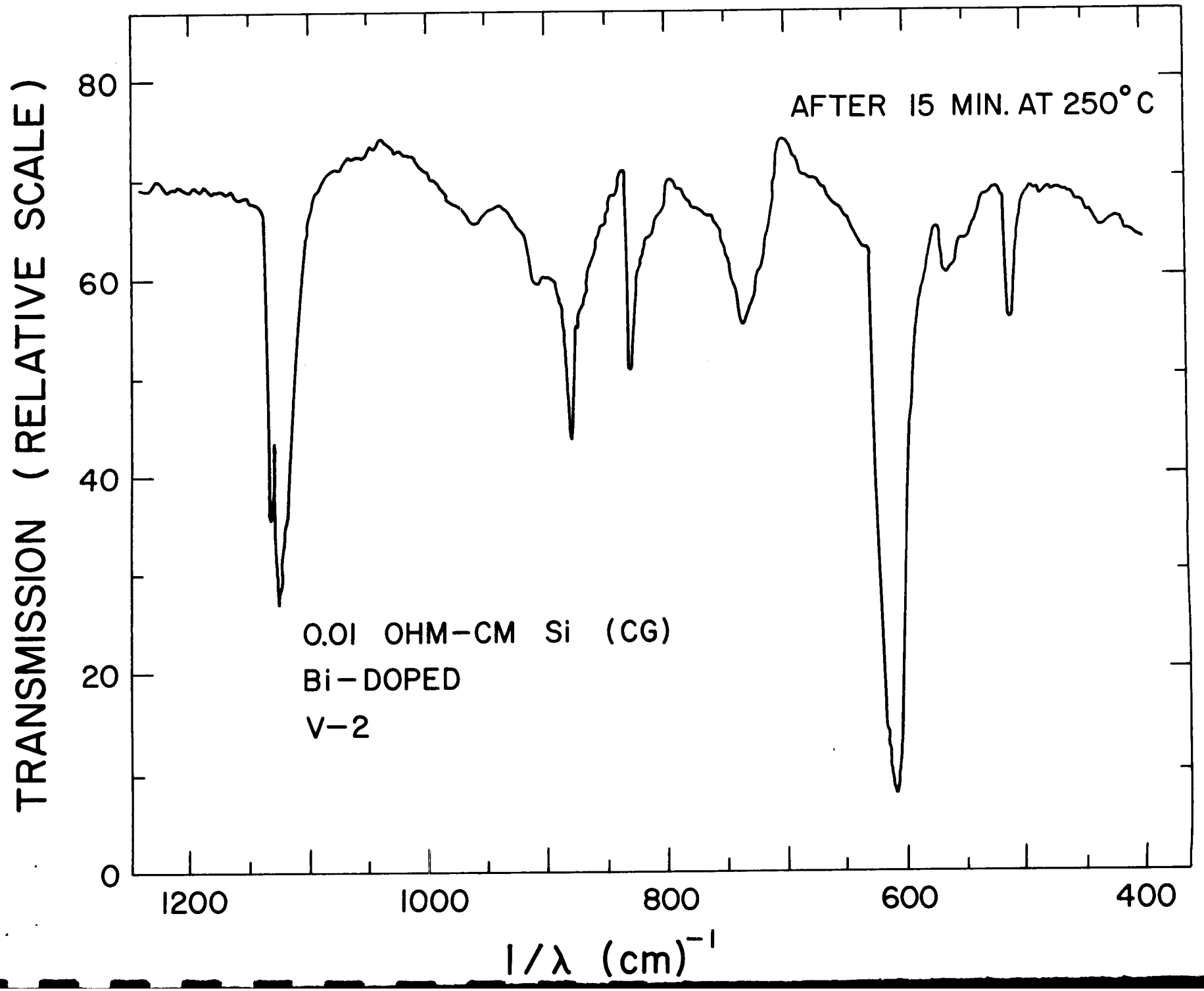
TRANSMISSION (RELATIVE SCALE)
80
60
40
20
0
AFTER 15 MIN. AT 250°C
0.01 OHM-CM Si (CG)
Bi-DOPED
V-2
1200
1000
800
600
400
1/λ (cm)⁻¹

Fig 2)

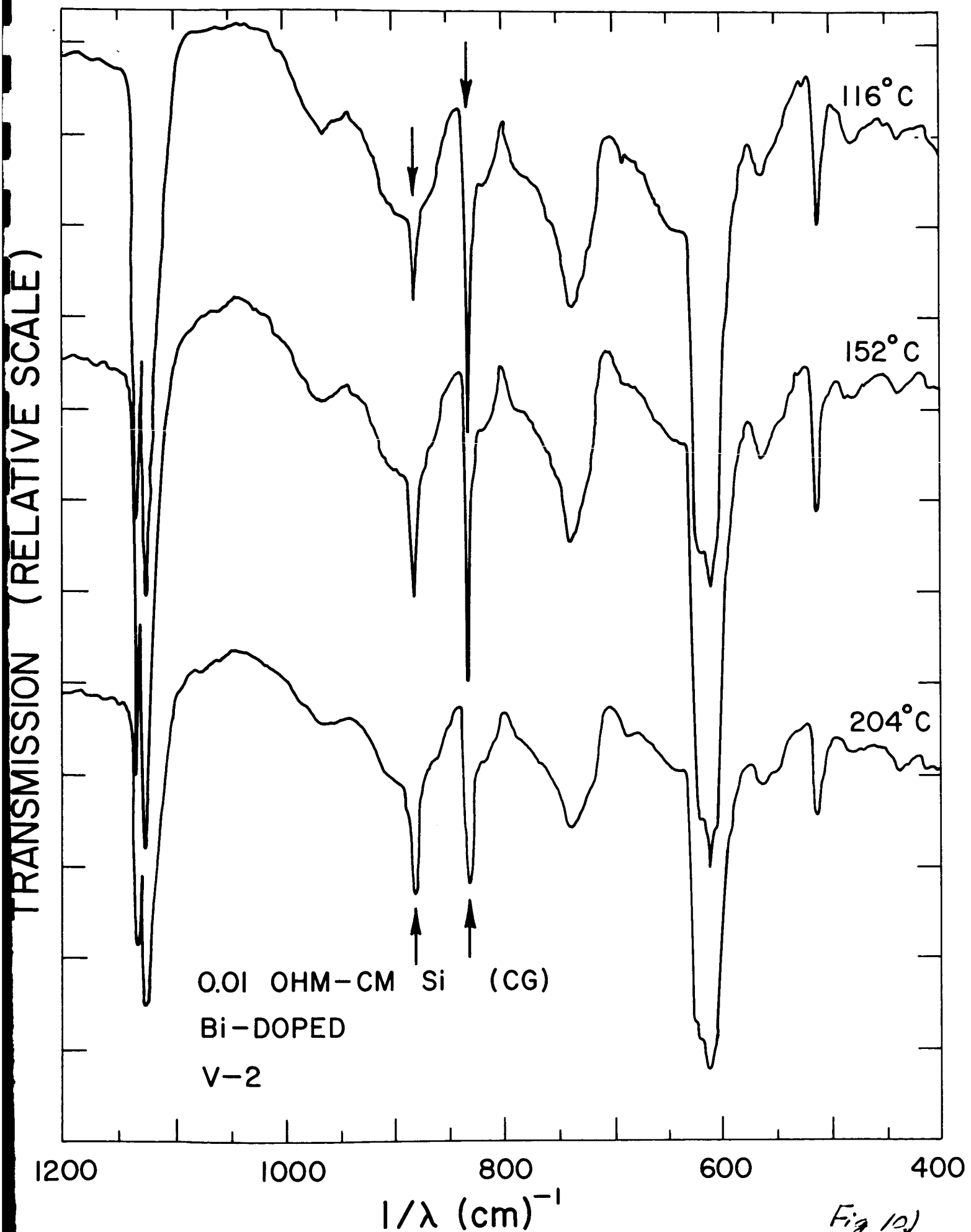
116°C
152°C
204°C
0.01 OHM-CM Si (CG)
Bi-DOPED
V-2
TRANSMISSION (RELATIVE SCALE)
1200
1000
800
600
400
1/λ (cm)⁻¹

Fig 12

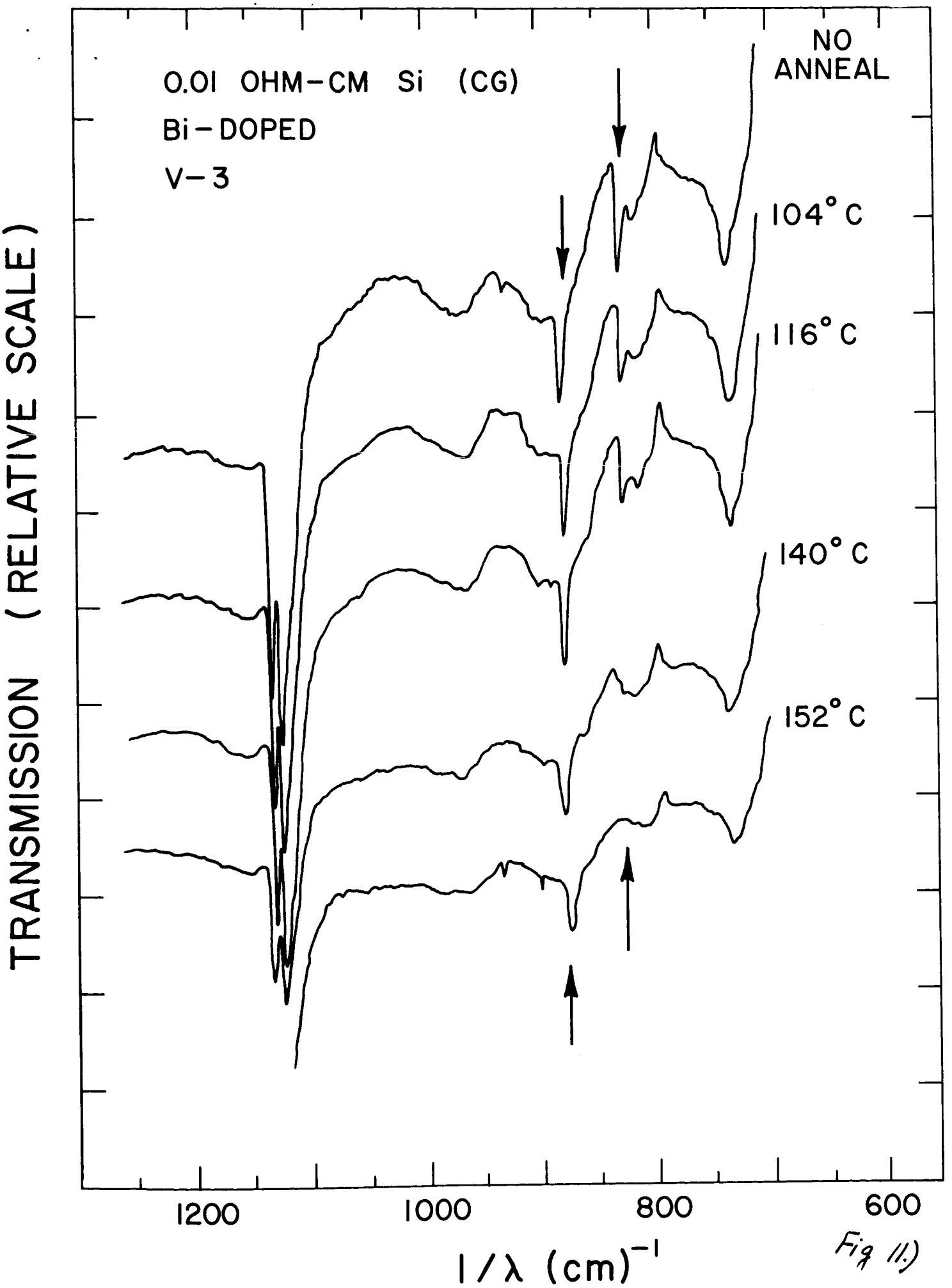
0.01 OHM-CM Si (CG)
Bi-DOPED
V-3
NO ANNEAL
104° C
116° C
140° C
152° C
TRANSMISSION (RELATIVE SCALE)
1200
1000
800
600
1/λ (cm)⁻¹

Fig 11.)